Title

Stabilizing the Meniscus for Operando Characterization of Platinum During the Electrolyte-Consuming Alkaline Oxygen Evolution Reaction

Journal

Topics in Catalysis, 61(20)

ISSN

1022-5528

Authors

Stoerzinger, Kelsey A

Favaro, Marco

Ross, Philip N

et al.

Publication Date

2018-12-01

DOI

10.1007/s11244-018-1063-6

Peer reviewed

Stabilizing the Meniscus for *Operando* Characterization of Platinum during the Electrolyte-Consuming Alkaline Oxygen Evolution Reaction

Kelsey A. Stoerzinger,[1,†] Marco Favaro,[2,3,4,†,‡] Philip N. Ross[5], Zahid Hussain[2], Zhi Liu[7,8], Junko Yano[3,6], Ethan J. Crumlin[2,9,*]

[1]*Physical and Computational Sciences Directorate, Pacific Northwest National Laboratory, Richland, WA 99352 USA*

[2]*Advanced Light Source, Lawrence Berkeley National Laboratory, One Cyclotron Rd, Berkeley, CA 94720, USA.*

[3]*Joint Center for Artificial Photosynthesis, Lawrence Berkeley National Laboratory, One Cyclotron Rd, Berkeley, CA 94720, USA*

[4]*Chemical Sciences Division, Lawrence Berkeley National Laboratory, One Cyclotron Rd, Berkeley, CA 94720, USA*[5]*Materials Sciences Division, Lawrence Berkeley National Laboratory, One Cyclotron Rd, Berkeley, CA 94720, USA*

[6]*Molecular Biophysics and Integrated Bioimaging Division, Lawrence Berkeley National Laboratory, One Cyclotron Rd, Berkeley, CA 94720, USA*

[7]*State Key Laboratory of Functional Materials for Informatics, Shanghai Institute of Microsystem and Information Technology, Chinese Academy of Sciences, Shanghai 200050, People's Republic of China*

[8]*Division of Condensed Matter Physics and Photon Science, School of Physical Science and Technology, ShanghaiTech University, Shanghai 200031, China*

[9]*Joint Center for Energy Storage Research, Lawrence Berkeley National Laboratory, One Cyclotron Rd, Berkeley, CA 94720, USA*

Corresponding Author

*ejcrumlin@lbl.gov; Tel. +1-510-486-6235

Present Addresses

[†]These authors contributed equally
[‡]Present address: Helmholtz Zentrum Berlin für Materialien und Energie GmbH, Institute for Solar Fuels, Hahn-Meitner-Platz 1, D-14109 Berlin, Germany

ORCID

KAS 0000-0002-3431-8290
MF 0000-0002-3502-8332

EJC 0000-0003-3132-190X

ABSTRACT

Achieving a molecular-level understanding of interfacial (photo)electrochemical processes is essential in order to tailor novel and highly-performing catalytic systems. The corresponding recent development of *in situ* and *operando* tools has posed new challenges on experimental architectures. In this study, we use ambient pressure X-ray photoelectron spectroscopy (AP-XPS) to probe the solid/liquid electrified interface of a polycrystalline Pt sample in contact with an alkaline electrolyte during hydrogen and oxygen evolution reactions. Using the “dip–and-pull” technique to probe the interface through a thin liquid layer generated on the sample surface, we observe that the electrolyte meniscus becomes unstable under sustained driving of an electrolyte-consuming reaction (such as water oxidation). The addition of an electrochemically inert supporting electrolyte mitigates this issue, maintaining a stable meniscus layer for prolonged reaction times. In contrast, for processes in which the electrolyte is replenished in the reaction pathway (i.e. water reduction in alkaline conditions), we find that the solid/liquid interface remains stable without addition of a secondary supporting electrolyte. The approach described in this work allows the extension of *operando* AP-XPS capabilities using the “dip-and-pull” method to a broader class of reactions consuming ionic species during complex interfacial faradaic processes.

KEYWORDS

Ambient Pressure XPS, Electrocatalysis, Oxygen Evolution Reaction, Hydrogen Evolution Reaction, Solid/liquid interface stability.

1. Introduction

The evolution of oxygen gas from a catalyst surface is a critical component in numerous industrial processes [1,2], ranging from the chlor-alkali process [3,4] to the electrotwinning of metals [5]. Such systems require not only catalysts which are efficient, cost-effective, and durable, but also the design of the electrochemical interface. *Operando* techniques contribute to this goal by probing the structure and composition of the dynamic electrified solid/liquid interface [6-12]. Of particular interest is the model system of platinum metal, that while scarce and expensive [13], can shed light on surface chemical and structural transformations under various (electro)chemical reaction environments. The detailed study of Pt aims to expedite the development of less costly and more abundant alternatives with tailored physical/chemical properties that surpass current state of the art, in particular for alkaline electrocatalysts [14-16].

X-ray photoelectron spectroscopy (XPS) is well-suited to probe electrochemical systems, as the binding energy (BE) of ejected photoelectrons is a function of the Galvani potential at the position of the atom undergoing photoionization. Furthermore, the technique can provide quantitative information regarding the composition and chemistry near the sample surface [17]. In contrast to typical ultrahigh vacuum surface science approaches, ambient pressure XPS (AP-XPS) enables the sample to be kept

at higher pressures [7,18]. Coupled with a “tender” X-ray (2-8 keV) source, AP-XPS can probe through a liquid layer tens of nanometer thick to reach a buried solid/liquid interface and thereby provide *operando* insight into the electrochemically active surface [19,20]. This can be achieved by the “dip-and-pull” technique [19,20], where electrodes are immersed into a liquid electrolyte and partially withdrawn at a constant rate, analyzing the region where a thin meniscus of electrolyte covers the electrode surface. The success of this approach hinges in part on the maintenance of a stable meniscus during operation, typically limiting it’s utility to low current densities [21] and electrodes of moderately hydrophilic character.

We have recently employed AP-XPS with “tender” X-rays ($h\nu$ = 4 keV) to study the prototypical Pt electrode for the water splitting reactions in alkaline electrolyte [22,23]. Though commercial alkaline electrolyzers are designed to operate in an electrolyte consisting solely of a highly concentrated KOH electrolyte [24,25], *operando* AP-XPS investigations can be hindered by the consumption of hydroxyl species during the oxygen evolution reaction (OER), which destabilizes the meniscus. We here employ a secondary supporting electrolyte to stabilize the meniscus during faradaic processes involving consumption of the electrolyte.

2. Methods

2.1 “Dip-and-pull” method and *operando* measurements. MilliQ water (DI, ρ = 18.2 MΩ cm) was used as the solvent, to which potassium hydroxide (KOH, 99.99%, Aldrich) and/or potassium fluoride (KF, 99.99%,

Aldrich) were added as the (supporting) electrolyte at concentrations of 1.0 or 0.1 M. All the potentials reported in this work are relative to the miniaturized leakless Ag/AgCl/Cl^- $_{(sat.)}$ (ET072-1, eDAQ) reference electrode (RE), with a standard electrode potential $E°_{Ag/AgCl(sat.)}$ = 197 mV with respect to the normal hydrogen electrode, NHE. Polycrystalline Pt foils (99.99%, thickness 0.5 mm, Aldrich) were used as the working electrode (WE) and counter electrode (CE), polished to a mirror finish with silicon carbide papers of decreasing grain size (Struers, grit: 2400 and 4000) and then ultrasonic cleaned in a mixture of MilliQ water:ethanol (Aldrich, 1 : 1) for 10 min, two times. The foils were then ultrasonic cleaned in pure MilliQ water for 15 min, followed by a thoroughly rinsing and drying in N_2 stream.

The WE, RE, and CE were mounted into a PEEK electrode housing, with electrical feedthrough to an external potentiostat/galvanostat (Biologic SP 300). The WE and the analyzer front cone shared a common ground. The electrolyte was outgassed prior to introduction into the experimental chamber at low pressure (~10 Torr) in a dedicated offline chamber for > 30 min. Once placed into the AP-XPS experimental chamber, the pressure was carefully lowered down to the water vapor pressure at room temperature, ~16 Torr.

The three electrodes were immersed into the electrolyte, then slowly extracted from the electrolyte solution by rising the manipulator at a constant vertical rate to produce a thin layer of liquid electrolyte film remaining on the Pt electrode (typically 10-30 nm thick) above the bulk

electrolyte, keeping the bottom of the electrodes immersed in the bulk electrolyte. The meniscus region was then moved to the focal point of the analyzer for AP-XPS investigation of the solid/liquid interface as a function of the applied potential.

An electrochemical cleaning procedure was conducted in the experimental chamber, prior to meniscus formation, by holding the Pt WE at −1200 mV for 30 minutes, in order to obtain a pure metallic and a homogeneous surface. Survey spectra (**Figure S1**) verify no unexpected elements are present on the Pt electrode or in the electrolyte. All cyclic voltammetry measurements were conducted at a scan rate of 50 mV s^{-1} (**Figure S2**). The WE was held potentiostatically at OER and hydrogen evolution reaction (HER) conditions during AP-XPS collection.

2.2 Beamline 9.3.1 and AP-XPS experimental details. Beamline 9.3.1 at the Advanced Light Source (ALS, Lawrence Berkeley National Laboratory) is equipped with a bending magnet and a Si (111) double crystal monochromator (DCM) having a total energy range between 2.0 keV and 7.0 keV [19,20,22,26,27]. The minimal spot size at the beamline is 0.7 mm (w) x 1.0 mm (h), and a constant photon energy of 4 keV was used throughout the experiment. The pass energy of the Scienta analyzer (R4000 HiPP-2) was set to 200 eV while the width of the entrance slit placed between the pre-lenses and the Herzog plate was set to 500 µm. The total resolution (X-rays and analyzer) was measured acquiring the Fermi edge on a clean gold polycrystalline sample, which provided a value of 460 meV for this

experiment. For the spectral acquisitions, we used a kinetic energy step of 100 meV and a dwell time of 300 µs. To limit the evaporation from the electrochemical cell, a larger outgassed water source was placed in the analysis chamber to provide a buffer.

Spectral fitting was carried out using CasaXPS, employing a Shirley background (**Table S1**). The binding energy (BE) scale was calibrated such that the metallic Pt^0 $4f_{7/2}$ photoelectron peak, fit with a Doniach–Šunjić shape, was at 71.2 eV [22]. The O1s spectra were fit with three 25:75 Lorentzian:Gaussian symmetrical approximations to the Voigt function: gas phase water (GPW), liquid phase water (LPW, including chemisorbed water), and a component encompassing surface oxygenated species at lower BE. The K 2p and F 1s spectra were also fit with symmetrical Voigt function approximations.

3. Results and Discussion

The Pt electrode/electrolyte interface was studied by AP-XPS in *operando*—as a function of applied potential at a solid/liquid interface—as shown in **Figure 1**. Employing a photon energy of 4 keV enables the "dip-and-pull" procedure [19,20,22,26,27] to simultaneously characterize ~20 nm of an aqueous electrolyte and ~10 nm of the Pt WE [22] while driving electrochemical reactions at the solid/liquid interface. The potential of the polycrystalline Pt WE (sharing a common ground with the analyzer) was controlled relative to the Ag/AgCl/$Cl^-_{(sat.)}$ RE, and the current balanced by the CE in the three electrode electrochemical cell. The experiments were

performed at a temperature and pressure of about 298 K and 18 Torr, respectively. The relative humidity (RH) was around 76 % (taking the equilibrium water vapor tension at 298 K as 23.7 Torr [28]).

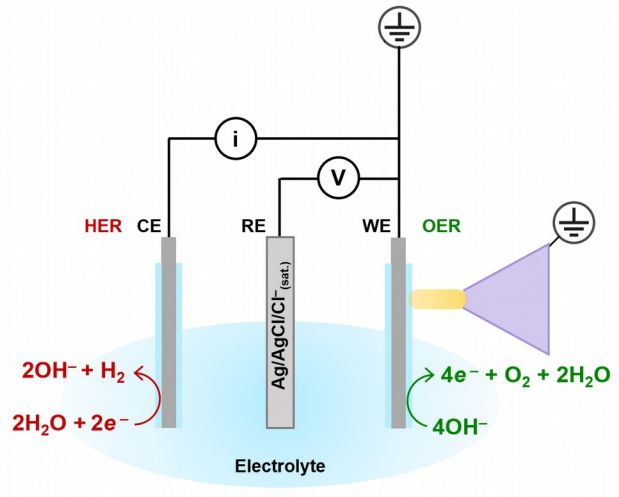

Figure 1. Schematic of the *operando* AP-XPS set-up at beamline 9.3.1 at the Advanced Light Source. The manipulator holds the Pt counter electrode (CE), reference electrode (RE), and Pt working electrode (WE). Anodic polarization, shown here at the WE, drives the oxygen evolution reaction (OER) and consumption of the electrolyte, while cathodic polarization, shown here at the CE, drives the hydrogen evolution reaction (HER) and replenishes the electrolyte.

We here compare the solid/liquid electrified interface for two reactions: the OER ¿, and the hydrogen evolution reaction, HER ¿. Both reactions generate gaseous products. In particular, in alkaline electrolyte (pH > 7), HER consumes the solvent H_2O to replenish the electrolyte with hydroxyls, whereas the OER consumes the hydroxyl anions. The charged species of the electrolyte (e.g. K^+, OH^-) are responsible for maintaining sufficient

conductivity such that the applied voltage drop is localized at the solid/liquid interface, and in the case of hydroxyls, also determines the electrolyte pH.

In contrast to commercial electrolyzers [24,29] or well-mixed large-volume cells typical used to assess catalytic activity [30], measurement in a meniscus configuration puts unique constraints on ionic transport [31-33], particularly for reactions such as the OER which consume the electrolyte. Even so, our previous investigation of the surface of Pt during alkaline OER at +0.9 V vs. the Ag/AgCl RE [22] exhibited stable surface chemistry and electrolyte distribution over two hours of cycling.

After two hours of OER in 1.0 M KOH electrolyte, however, the meniscus layer through which the photoelectrons pass became unstable. The photoelectron peak from liquid phase water (LPW) in the O 1s shifted to higher BE, indicating a loss in anodic polarization in the meniscus region probed by AP-XPS, mirrored by the K 2p (**Figure 2**). Simultaneously, a reduction in the intensity of the LPW compared to the gas phase water (GPW) photoelectrons indicated thinning of the meniscus, coupled with a decrease in K intensity (**Figure 2c**). The instability of the meniscus layer upon prolonged polarization is hypothesized to result from an electrowetting effect and/or consumption of the hydroxyl species during OER. High local depletion rates of OH^- anions and coupled migration of K^+ species into the bulk electrolyte sink can exceed the diffusion of OH^- and subsequent K^+ ions (due to electron neutrality) back into the meniscus to replenish those which are being consumed or repelled away from the solid/liquid interface probed

by AP-XPS. Eventually, this leads to breakup of the meniscus layer and loss of applied potential. This hypothesis is supported by the fact that for HER [23], a reaction which also forms gas bubbles but replenishes OH^- anions via the reduction of H_2O to H_2, the O 1s and K 2p remain stable, even after more than two hours of cycling (**Figure 2** d-f). The stability during HER further suggests meniscus collapse is not driven by evaporation or pH gradients alone. However it is worth noting that H_2O has a larger molar concentration, 55:1 compared to KOH, and can be sourced via condensation from the vapor phase (which is at about 76 % RH) as well as diffusion from the bulk electrolyte source.

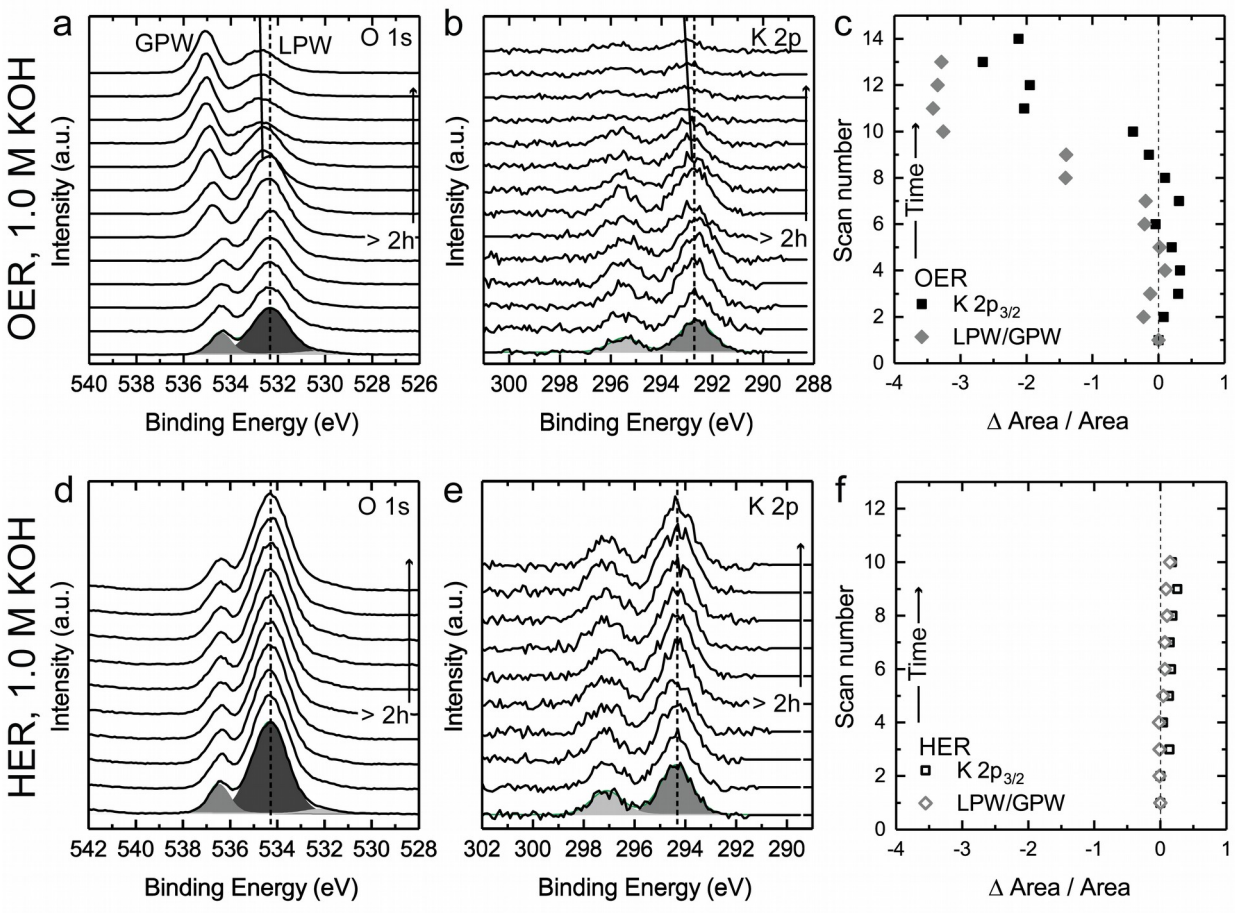

Figure 2. *Operando* AP-XPS in 1.0 M KOH. During OER [22] at +0.9 V vs Ag/AgCl, the (a) O 1s and (b) K 2p change dramatically after two hours, with liquid phase water (LPW) and K decreasing in intensity and shifting to higher binding energy, and the gas phase water (GPW) increasing. (c) The relative decrease in K $2p_{3/2}$ area and LPW/GPW ratio (where Δ Area/Area represents the change in integrated area (K $2p_{3/2}$) or area ratio (LPW/GPW) relative to the initial scan, normalized to that of the noted scan) indicate that the meniscus thickness decreases after 2 h of OER. During HER [23] at −0.9 V vs Ag/AgCl, the (d) O 1s and (e) K 2p are similar over time, and (f) show negligible relative change in areas relative to the first scan, indicating the meniscus is stable. Spectra in (a), (b), and (d) are Shirley-background

subtracted, and all spectra are offset for clarity. Representative fits to the spectra are provided for the initial scan, detailed in Table S1.

In order to stabilize the meniscus layer, enabling tender AP-XPS during prolonged measurement of electrolyte-consuming reactions such as alkaline OER and to work towards reaching higher current densities, we employ a secondary supporting electrolyte. The non-interacting salt serves to regulate cell resistance and mass transport by electrical migration and can notably influence the structure of the double layer [34]. We add 0.1 M KF to the 1.0 M KOH electrolyte, where F^- is not reported to notably influence the potentials of OER in well-mixed rotating disk electrode cells [35] or influence adsorption on Pt in aqueous solutions [36], in contrast with chloride anions [37]. A lowering of the onset potential during OER is observed in the meniscus configuration is observed upon addition of KF (**Figure S2**), leading to subtle changes in the Pt 4f probed at comparable current densities (**Figure S3**) and motivating further studies of the double layer structure and surface speciation in F^- containing electrolytes. The addition of the supporting electrolyte stabilizes the meniscus layer far beyond 2 h of OER (**Figure 3**). The liquid electrolyte layer and the K^+ intensity is maintained, and the applied voltage remains constant, illustrating control over the local potential during prolonged *operando* characterization. Some variation in intensity is occasionally observed, potentially from salt in the nose cone. The overpotential required to drive OER at comparable rates decreased upon addition of 0.1 M KF, potentially arising from improved conductivity through

the thin capillary, thus the electrode is polarized to lower potentials of +0.75 V vs. Ag/AgCl (**Figure S2**).

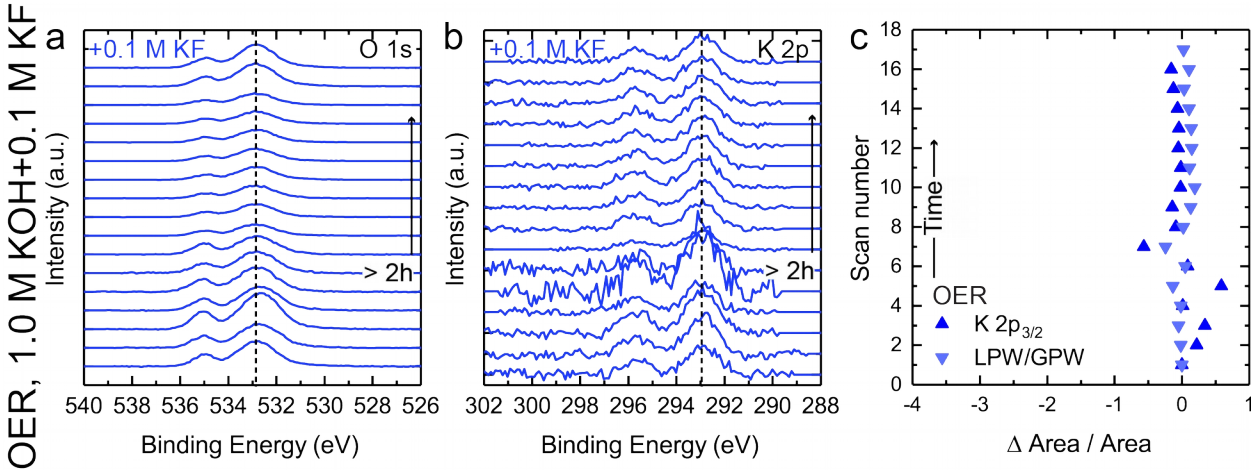

Figure 3. *Operando* AP-XPS in 1.0 M KOH with 0.1 M KF. During OER at +0.75 vs. Ag/AgCl, the (a) O 1s and (b) K 2p spectra remain similar, including after two hours. (c) The relative change in K $2p_{3/2}$ area and LPW/GPW ratio (compared to the first scan) is negligible, indicating that adding KF to the electrolyte stabilizes the meniscus. Spectra are Shirley-background subtracted and offset for clarity.

We confirm the KF supporting electrolyte does not interact with the Pt electrode by performing the water splitting reactions in a solution containing only 1.0 M KF (no KOH). In order to obtain comparable rates for OER in the approximately neutral solution, a larger anodic potential relative to Ag/AgCl is required (**Figure S2**). Driving OER at +1.25 V vs Ag/AgCl, the meniscus remains stable far beyond 2 h of polarization, exhibiting a constant intensity of the LPW peak in the O 1s, as probed by AP-XPS (**Figure 4**). The Pt 4f is somewhat more oxidized compared to in 1.0 M KOH or 1.0 M KOH+0.1 M KF

only (**Figure S4**), but remains unchanged overtime, suggesting no reaction between the KF supporting electrolyte and Pt at the applied potentials. The intensity of the K 2p and F 1s also remain constant with time, indicating that the non-interacting salt provides sufficient ionic conductivity to balance the consumption of H^+/OH^- during OER in neutral solutions. The singular BE in the symmetric F 1s (**Figure S5**) indicates the F^- is not specifically adsorbed to the grounded Pt surface, but instead shifts with the Galvani potential.

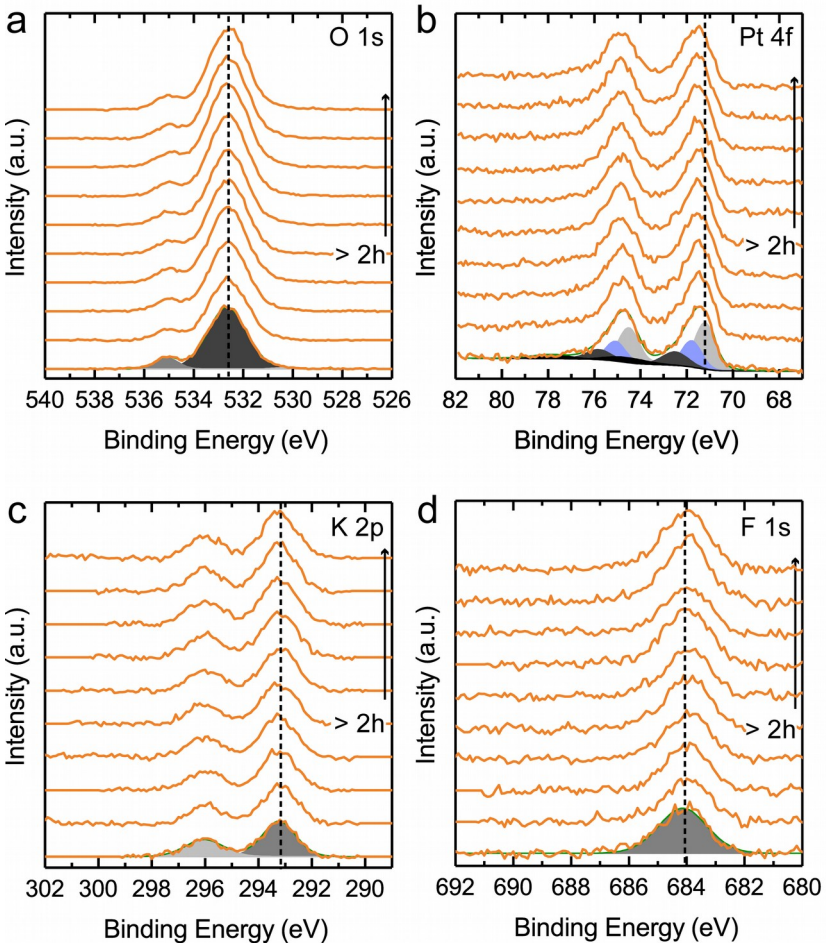

Figure 4. *Operando* AP-XPS in 1.0 M KF (no KOH). During OER, the (a) O 1s, (b) Pt 4f, (c) K 2p, and (d) F 1s spectra remain similar, including after two hours. This indicates the meniscus is stable during OER due to the presence

of non-interacting K^+ and F^- ions. Spectra in (a), (c), and (d) are Shirley-background subtracted and all are offset for clarity. Representative fits to the spectra are provided for the initial scan, detailed in Table S1.

Similar behavior is observed for the HER in 1.0 M KF (**Figure 5**), where the Pt 4f is comparable to that for HER in KOH (**Figure S4**). Compared to OER conditions, the K 2p and F 1s shift to higher BE as expected for solution species compared to a WE held at more cathodic conditions, supporting the non-interacting nature of the salt. The intensity and BE of the ionic species are constant over time, indicating that the meniscus remains stable far beyond 2 h in *operando*.

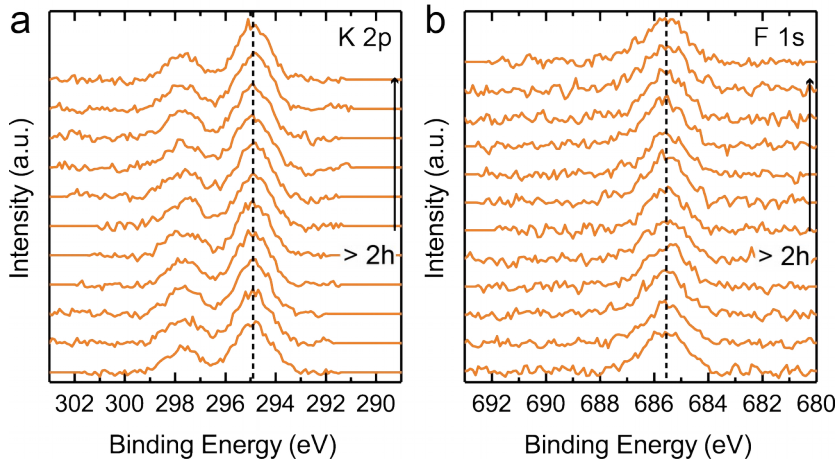

Figure 5. *Operando* AP-XPS in 1.0 M KF (no KOH). During HER, the (a) K 2p and (b) F 1s spectra remain similar, including after two hours, indicating K^+ and F^- ions do not interact with the surface and that the meniscus remains stable. Spectra are Shirley-background subtracted and offset for clarity.

The behavior of ionic species in the meniscus during OER and HER can be quantified by both the BE (“position”) and the integrated intensity (“area”) of

the core level (**Figure 6**). While K^+ ions initially remain at constant BE and intensity in all cases, driving OER in an electrolyte consisting solely of 1.0 M KOH leads to the onset of meniscus breakup after ~2 h (scan 6). The shift to higher BE indicates a loss of anodic polarization, hypothesized to be driven by a thinning of the meniscus – evident by the reduction in K^+ and LPW (**Figure 2**) intensity – from consumption of OH^- species during the OER. This behavior is not observed for HER in 1.0 M KOH, where the reaction replenishes OH^- species. The inclusion of a supporting electrolyte of non-interacting KF salt stabilizes the meniscus for both OER and HER, and both K^+ and F^- maintain a constant profile in the meniscus during the reaction.

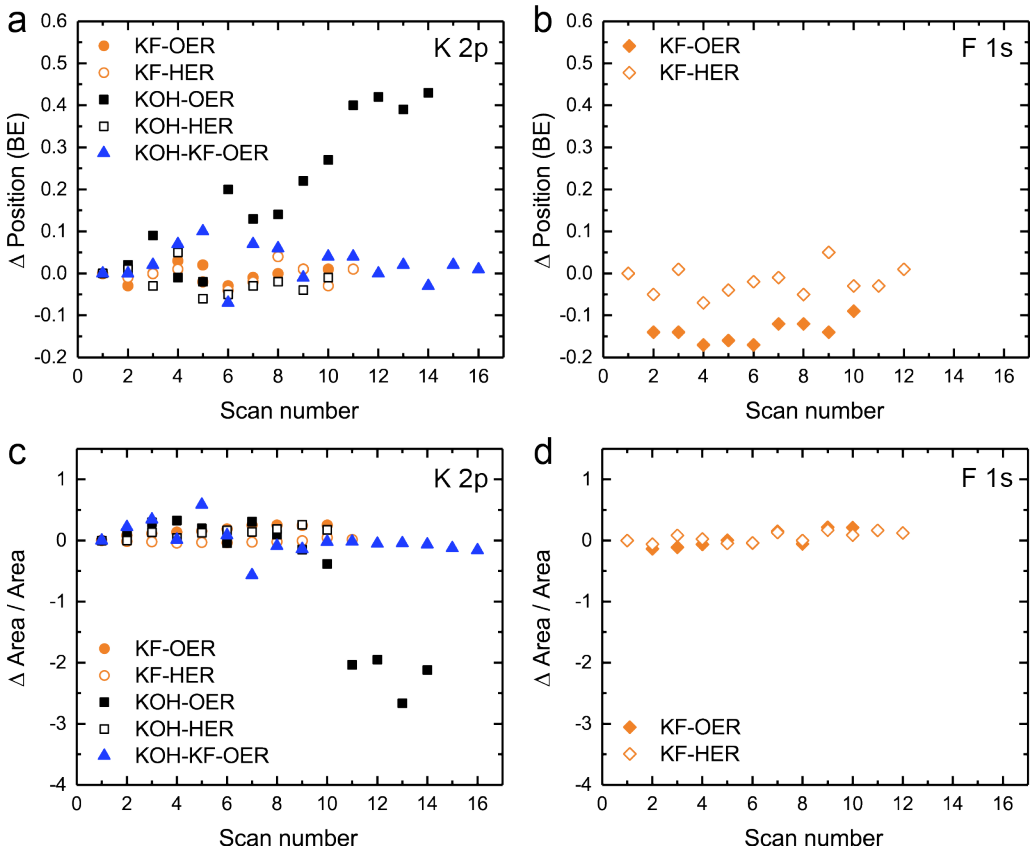

Figure 6. Quantification of changes in location and amount of ionic species. Change in position for (a) K 2p and (b) F 1s relative to the initial scan. For OER in an electrolyte containing only 1.0 M KOH, instability of the meniscus leads to an increase in BE and a loss of polarization. The change in (c) K $2p_{3/2}$ and (d) F 1s area compared to the initial scan, normalized by the area. For OER in an electrolyte containing only 1.0 M KOH, instability of the meniscus leads to a local decrease in K^+ from consumption of OH^- and thinning of the meniscus.

4. Conclusions

We employed AP-XPS using a “tender” X-ray source (4 keV) to probe the Pt/electrolyte interface in *operando* during alkaline water splitting reactions. The meniscus configuration of the region probed by AP-XPS has typically constrained the conditions to ones of low current densities and reactions not involving the consumption of electrolyte. For example, we here showed that the conversion of OH^- to O_2 and H_2O during alkaline OER depletes the meniscus of charged species (**Figure 7**), leading to collapse of the meniscus and loss of polarization control at the region of interest. This is in contrast to the HER, which replenishes OH^- during the generation of H_2 from H_2O, maintaining the ionic strength and conductivity within the meniscus, which remains stable. We here demonstrated that the meniscus can be stabilized during OER by the addition of a supporting electrolyte of non-interacting salt. The addition of 0.1 M KF to the 1.0 M KOH electrolyte provided additional

charged species to the meniscus, stabilizing the double layer and maintaining ionic transport. This approach enables the study of electrolyte-consuming reactions with *operando* AP-XPS using the "dip-and-pull" approach to gain new insight into the electrified solid/liquid interface. Extending this experimental strategy to earth abundant materials will aid in the rational design of novel tailored materials for water splitting reactions in alkaline.

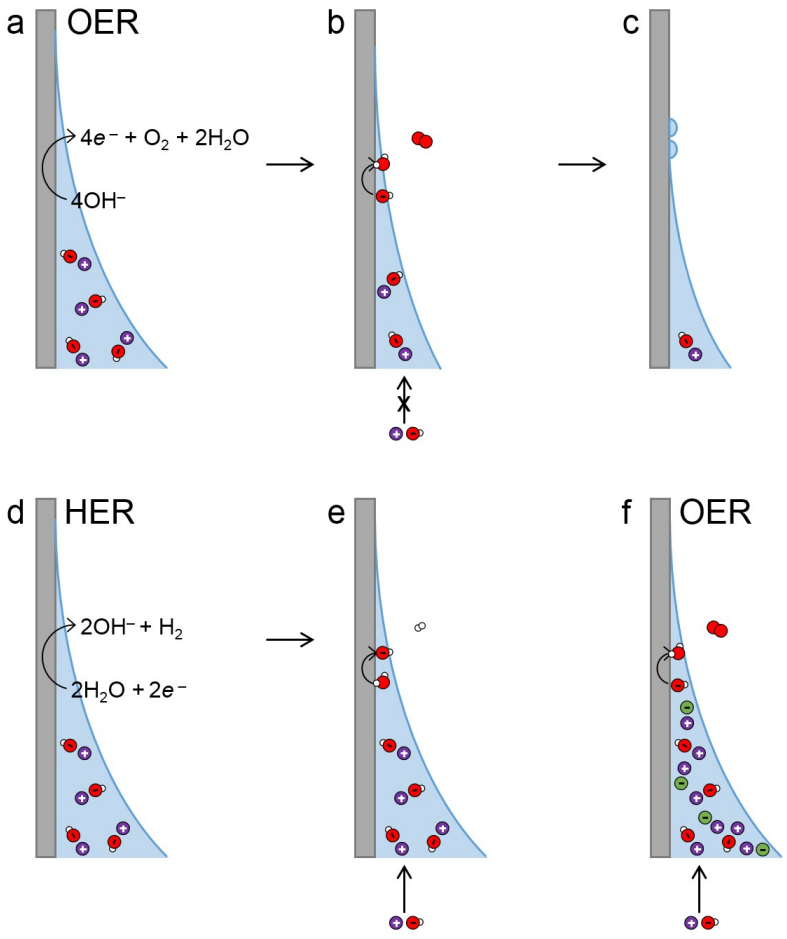

Figure 7. Simplified schematic illustrating the electrolyte species present during the noted reaction and whether the meniscus is stable or collapses. (a) OER consumes OH^-, the only anion in 1.0 M KOH. This consumption leads to (b) electrolyte depletion in the destabilized meniscus, which (c) collapses, leading to some regions of discontinuity. (d) HER produces OH^-, consuming the abundant H_2O solvent in 1.0 M KOH, and (e) the meniscus remains stable and maintains sufficient ionic transport. (f) For OER, adding a supporting electrolyte of 0.1 M KF to the 1.0 M KOH introduces additional F^- anions (green, and more K^+ cations, purple) which are not consumed in the reaction. The meniscus remains stable and maintains sufficient ionic transport.

ACKNOWLEDGMENT

This work was partially supported through the Office of Science, Office of Basic Energy Science (BES), of the U.S. Department of Energy (DOE) under award no. DE-SC0004993 to the Joint Center for Artificial Photosynthesis (JCAP), a DOE Energy Innovation Hub. The Advanced Light Source is supported by the Director, Office of Science, Office of Basic Energy Sciences, of the U.S. DOE under Contract No. DE-AC02-05CH11231. K.A.S. gratefully acknowledges support from the Linus Pauling Distinguished Post-Doctoral Fellowship Pacific Northwest National Laboratory (PNNL, Laboratory Directed Research and Development Program 69319). PNNL is a multiprogram national laboratory operated for DOE by Battelle.

Supporting Information. *Additional figures, fitting parameters.*

REFERENCES

1. Reier T, Nong HN, Teschner D, Schlögl R, Strasser P (2017) Electrocatalytic oxygen evolution reaction in acidic environments – reaction mechanisms and catalysts. Adv Energy Mat 7 (1):1601275

2. Cherevko S, Geiger S, Kasian O, Kulyk N, Grote J-P, Savan A, Shrestha BR, Merzlikin S, Breitbach B, Ludwig A, Mayrhofer KJJ (2016) Oxygen and hydrogen evolution reactions on Ru, RuO_2, Ir, and IrO_2 thin film electrodes in acidic and alkaline electrolytes: A comparative study on activity and stability. Catal Today 262 (Supplement C):170-180

3. Karlsson RKB, Cornell A (2016) Selectivity between oxygen and chlorine evolution in the Chlor-Alkali and Chlorate processes. Chem Rev 116 (5):2982-3028

4. Trasatti S (1984) Electrocatalysis in the anodic evolution of oxygen and chlorine. Electrochim Acta 29 (11):1503-1512

5. Clancy M, Bettles CJ, Stuart A, Birbilis N (2013) The influence of alloying elements on the electrochemistry of lead anodes for electrowinning of metals: A review. Hydrometallurgy 131-132 (Supplement C):144-157

6. Carpenter BK, Harvey JN, Orr-Ewing AJ (2016) The study of reactive intermediates in condensed phases. J Am Chem Soc 138 (14):4695-4705

7. Crumlin EJ, Liu Z, Bluhm H, Yang W, Guo J, Hussain Z (2015) X-ray spectroscopy of energy materials under in situ/operando conditions. J Electron Spectrosc Relat Phenom 200:264-273

8. Kaya S, Ogasawara H, Näslund L-Å, Forsell J-O, Casalongue HS, Miller DJ, Nilsson A (2013) Ambient-pressure photoelectron spectroscopy for heterogeneous catalysis and electrochemistry. Catal Today 205:101-105

9. Kornienko N, Resasco J, Becknell N, Jiang C-M, Liu Y-S, Nie K, Sun X, Guo J, Leone SR, Yang P (2015) Operando spectroscopic analysis of an amorphous cobalt sulfide hydrogen evolution electrocatalyst. J Am Chem Soc 137 (23):7448-7455

10. Ramaker DE, Korovina A, Croze V, Melke J, Roth C (2014) Following ORR intermediates adsorbed on a Pt cathode catalyst during break-in of a PEM fuel cell by in operando X-ray absorption spectroscopy. Phys Chem Chem Phys 16 (27):13645-13653

11. Schlögl R (2015) Heterogeneous catalysis. Angew Chem Int Ed 54 (11):3465-3520

12. Zandi O, Hamann TW (2016) Determination of photoelectrochemical water oxidation intermediates on haematite electrode surfaces using operando infrared spectroscopy. Nat Chem 8 (8):778-783

13. Vesborg PCK, Jaramillo TF (2012) Addressing the terawatt challenge: scalability in the supply of chemical elements for renewable energy. RSC Adv 2 (21):7933-7947

14. Fan J, Qi K, Zhang L, Zhang H, Yu S, Cui X (2017) Engineering Pt/Pd interfacial electronic structures for highly efficient hydrogen evolution and alcohol oxidation. ACS App Mater Interfaces 9 (21):18008-18014

15. Kavian R, Choi S-I, Park J, Liu T, Peng H-C, Lu N, Wang J, Kim MJ, Xia Y, Lee SW (2016) Pt-Ni octahedral nanocrystals as a class of highly active electrocatalysts toward the hydrogen evolution reaction in an alkaline electrolyte. J Mat Chem A 4 (32):12392-12397

16. Wang P, Zhang X, Zhang J, Wan S, Guo S, Lu G, Yao J, Huang X (2017) Precise tuning in platinum-nickel/nickel sulfide interface nanowires for synergistic hydrogen evolution catalysis. Nat Comm 8:14580

17. Fadley CS (2010) X-ray photoelectron spectroscopy: Progress and perspectives. J Electron Spectrosc Relat Phenom 178-179 (Supplement C):2-32

18. Stoerzinger KA, Hong WT, Crumlin EJ, Bluhm H, Shao-Horn Y (2015) Insights into Electrochemical Reactions from Ambient Pressure Photoelectron Spectroscopy. Acc Chem Res 48 (11):2976-2983

19. Axnanda S, Crumlin EJ, Mao B, Rani S, Chang R, Karlsson PG, Edwards MOM, Lundqvist M, Moberg R, Ross P, Hussain Z, Liu Z (2015) Using “tender” X-ray ambient pressure X-ray photoelectron spectroscopy as a direct probe of solid-liquid interface. Sci Rep 5:9788

20. Favaro M, Jeong B, Ross PN, Yano J, Hussain Z, Liu Z, Crumlin EJ (2016) Unravelling the electrochemical double layer by direct probing of the solid/liquid interface. Nat Comm 7:12695

21. Lewerenz H-J, Lichterman MF, Richter MH, Crumlin EJ, Hu S, Axnanda S, Favaro M, Drisdell W, Hussain Z, Brunschwig BS, Liu Z, Nilsson A, Bell AT, Lewis NS, Friebel D (2016) Operando analyses of solar fuels light absorbers and catalysts. Electrochim Acta 211 (Supplement C):711-719

22. Favaro M, Valero-Vidal C, Eichhorn J, Toma FM, Ross PN, Yano J, Liu Z, Crumlin EJ (2017) Elucidating the alkaline oxygen evolution reaction mechanism on platinum. J Mat Chem A 5 (23):11634-11643

23. Stoerzinger KA, Favaro M, Ross PN, Yang J, Liu Z, Hussain Z, Crumlin EJ (2017) Probing the surface of platinum during the hydrogen evolution reaction in alkaline electrolyte. J Phys Chem B 112 (2)864-870.

24. Santos DMF, Sequeira CAC, Figueiredo JL (2013) Hydrogen production by alkaline water electrolysis. Quim Nova 36:1176-1193

25. Esposito DV Membraneless electrolyzers for low-cost hydrogen production in a renewable energy future. Joule https://doi.org/10.1016/j.joule.2017.07.003

26. Eilert A, Cavalca F, Roberts FS, Osterwalder J, Liu C, Favaro M, Crumlin EJ, Ogasawara H, Friebel D, Pettersson LGM, Nilsson A (2017) Subsurface oxygen in oxide-derived copper electrocatalysts for carbon dioxide reduction. J Phys Chem Lett 8 (1):285-290

27. Lichterman MF, Hu S, Richter MH, Crumlin EJ, Axnanda S, Favaro M, Drisdell W, Hussain Z, Mayer T, Brunschwig BS, Lewis NS, Liu Z, Lewerenz H-J (2015) Direct observation of the energetics at a semiconductor/liquid

junction by operando X-ray photoelectron spectroscopy. Energy Environ Sci 8 (8):2409-2416

28. Haar L, Gallagher JS, Kell GS (eds) (1984) NBS/NRC Steam Tables. Hemisphere Publishing Corp., New York

29. Diéguez PM, Ursúa A, Sanchis P, Sopena C, Guelbenzu E, Gandía LM (2008) Thermal performance of a commercial alkaline water electrolyzer: Experimental study and mathematical modeling. Int J Hydrogen Energy 33 (24):7338-7354

30. McCrory CCL, Jung S, Peters JC, Jaramillo TF (2013) Benchmarking heterogeneous electrocatalysts for the oxygen evolution reaction. J Am Chem Soc 135 (45):16977-16987

31. Villullas HM, Lopez Teijelo M (1996) Meniscus shape and lateral wetting at the hanging meniscus rotating disc (HMRD) electrode. J Appl Electrochem 26 (3):353-359

32. Ali-Löytty H, Louie MW, Singh MR, Li L, Sanchez Casalongue HG, Ogasawara H, Crumlin EJ, Liu Z, Bell AT, Nilsson A, Friebel D (2016) Ambient-pressure XPS study of a Ni–Fe electrocatalyst for the oxygen evolution reaction. J Phys Chem C 120 (4):2247-2253

33. Favaro M, Abdi FF, Lamers M, Crumlin EJ, Liu Z, van de Krol R, Starr DE (2017) Light-induced surface reactions at the bismuth vanadate/potassium phosphate interface. J Phys Chem B https://doi.org/10.1021/acs.jpcb.7b06942

34. Dickinson EJF, Limon-Petersen JG, Rees NV, Compton RG (2009) How much supporting electrolyte is required to make a cyclic voltammetry

experiment quantitatively “diffusional”? A theoretical and experimental investigation. J Phys Chem C 113 (25):11157-11171

35. Hwang I, Ahn E, Tak Y (2014) Effect of flouride ions on oxygen reduction and evolution reaction at α-MnO_2 Cathode. Int J Electrochem Sci 9 (10):5454-5466

36. Soriaga MP, Chia VKF, White JH, Song D, Hubbard AT (1984) The orientation and electrochemical oxidation of hydroquinone chemisorbed on platinum electrodes in various weakly surface-active supporting electrolytes. J Electroanal Chem Interfacial Electrochem 162 (1):143-152

37. Garcia-Araez N, Climent V, Herrero E, Feliu J, Lipkowski J (2005) Thermodynamic studies of chloride adsorption at the Pt(111) electrode surface from 0.1 M $HClO_4$ solution. J Electroanal Chem 576 (1):33-41